Journal of Nuclear Materials 382 (2008) 210–216

Contents lists available at ScienceDirect

Journal of Nuclear Materials

journal homepage: www.elsevier.com/locate/jnucmat

Analysis of high temperature deformation mechanism in ODS EUROFER97 alloy

A. Ramar *, P. Spätig, R. Schäublin

Ecole Polytechnique Fédérale de Lausanne (EPFL), Center for Research in Plasma Physics, Association Euratom-Confédération Suisse, CH 5232 Villigen PSI, Switzerland

A B S T R A C T

Oxide dispersion in tempered martensitic EUROFER97 steel is an efficient approach to improve its strength. The oxide dispersion strengthened (ODS) EUROFER97 steel shows a good strength up to 600 °C, but degrades rapidly beyond that temperature. To understand the origin in the microstructure of this drop in strength in situ heating experiment in TEM was performed from room temperature to 1000 °C. Upon heating neither microstructure changes nor dislocation movement are observed up to 600 °C. Movement of dislocations are observed above 680 °C. Phase transformation to austenite starts at 840 °C. Yttria particles remain stable up to 1000 °C. Changes in mechanical properties thus do not relate to changes in yttria dispersion. It is attempted to relate these observations to the thermal activation parameters measured by the technique of conventional strain rate experiment, which allow to identify at a mesoscopic scale the microstructural mechanisms responsible for the degradation of ODS steel at high temperatures.

1. Introduction

Oxide dispersion strengthened (ODS) tempered martensitic steels appear to be promising candidates for the future fusion reactor. The good thermal conductivity, swelling resistance and low radiation damage accumulation of the tempered martensitic, are further enhanced by the presence of a fine dispersion of oxide particles. They would allow in principle for a higher operating temperature of the fusion reactor, which improves its thermal efficiency. In effect, their strength remains higher than the base material with increasing temperature [1–3]. Their creep properties are also improved relatively to the base material [4–6]. However, the improvement of their strength is usually done at the expense of their fracture properties. The base material is the tempered martensitic steel EUROFER97 with the chemical composition Fe, 8.9 wt% Cr, 1.1 wt% W, 0.47 wt% Mn, 0.2 wt% V, 0.14 wt% Ta and 0.11 wt% C [7,8]. A number of studies have shown that the mechanical properties of given tempered martensitic steels are indeed improved by the oxide dispersion and that they retain a better behavior at high temperatures.

It is well known that the mechanical properties of the EUROFER97 degrades rapidly above 500 °C [5,6]. While the addition of the oxide particles raises the upper limit of operation to 600 °C, the strength of the material degrades rapidly after 600 °C. In this study the high temperature deformation mechanism of the ODS EUROFER97 alloy is investigated in detail. Attempt is made to understand the mechanism of deformation at high temperature in relation to the thermal activation parameters. In situ TEM heating investigation would allow to observe the microstructure and yttria particle stability, to make sure that the thermal activation parameters calculated are from the similar type of microstructure over different temperatures. Also, several types of heat treatment were given to understand the microstructural stability of EUROFER97 having tempered martensite as its final resulting microstructure.

2. Experimental

ODS EUROFER97 with 0.3% of yttria dispersed in the matrix of EUROFER97 was delivered from FZK in Germany. The alloy was prepared through the classical powder metallurgical route and was further hot rolled into plates. The final heat treatment given to the alloy was normalization at 1100 °C for 30 min followed by air quenching and tempering at 780 °C for 2 h. For optical microscopy observations, the samples were mechanically polished up to fine alumina polishing and were electrolytically etched using the saturated oxalic acid solution with 15 V at room temperature. Transmission electron microscopy (TEM) observations were done on ODS alloy disks of 1 mm in diameter inserted in a 3 mm stainless steel disk and thinned using the jet polishing technique, at −2 °C with 20 V using the solution of 10% perchloric acid in 90% of ethanol [9]. The samples thinned to electron transparency were investigated in a JEOL 2010 electron microscope equipped with a LaB6 gun and a high tilt lens operated at 200 kV. Energy dispersive X-ray spectrometry (EDS) was used to distinguish the oxide particles from the carbides with an Oxford Si (Li) detector. To understand the thermal stability of the ODS matrix microstructure, the

* Corresponding author. Tel.: +41 56 310 2645.
E-mail address: amuthan.ramar@psi.ch (A. Ramar).

0022-3115/$ - see front matter © 2008 Elsevier B.V. All rights reserved.
doi:10.1016/j.jnucmat.2008.08.009

as-received EUROFER97 was heat treated at 400, 600 and 800 °C in vacuum for one hour followed by air quenching. In-situ TEM heating observation was done in a Gatan TEM double tilt sample holder equipped with a molybdenum furnace operating up to 1000 °C. During the in situ heating, carried out as an isothermal anneal experiment, observation of the microstructure was made at intervals of 100 °C and lasted about 15 min at each temperature step, starting at room temperature and finishing at 1000 °C. Heating ramp between temperature steps lasted about 30 s.

3. Analysis of thermal activation parameters

Uniaxial tensile test were performed on cylindrical samples prepared as per ASTM standard. Two initial nominal strain rates were used for tensile tests, namely $10^{-3}\,s^{-1}$ and $10^{-5}\,s^{-1}$. The tensile tests were done at room temperature, 200, 300, 400, 500, 600, 700 and 800 °C in Ar atmosphere. In order to assess the thermal activation parameters of dislocation rate controlling mechanisms, the applied uniaxial stress was converted into a shear stress, τ, responsible for dislocation motion. The shear stress, τ, was calculated from the ratio of the measured uniaxial tensile stress, σ, to the Taylor's factor, M, where Taylor's factor is 3 for bcc structures [15,17].

Assuming that a single operative rate controlling mechanism is active, the plastic strain rate can be described by an Arrhenius equation:

$$\dot{\gamma}_p = \dot{\gamma}_{po} \exp\left(-\frac{\Delta G}{kT}\right), \tag{1}$$

where k is the Boltzmann constant, T the absolute temperature and ΔG is the Gibbs free energy required by a dislocation to overcome a localized obstacle [10]. $\dot{\gamma}_p$ accounts in particular for dislocation vibrational frequency, and mobile dislocation density. The activation volume is derived from Eq. (2), which is a partial derivative of the Gibbs free energy to the shear stress [11,17],

$$V = \frac{-\partial \Delta G}{\partial \tau}. \tag{2}$$

The activation volume is usually expressed in b^3, where b is the Burgers vector of the $a_0/2\langle 1\,1\,1\rangle$ dislocation and is taken as 0.268 nm. Assuming that $\dot{\gamma}_{po}$ does not vary significantly during the stress and strain rate increment it can be expressed as

$$V = KT\left(\frac{\partial \ln(\gamma_p/\gamma_{po})}{\partial \tau}\right) \cong KT\left(\frac{\partial \ln \dot{\gamma}_p}{\partial \tau}\right) \cong KT\left(\frac{\Delta \ln \dot{\gamma}_p}{\Delta \tau}\right). \tag{3}$$

Thus V can be related to experimentally accessible relations between $\dot{\gamma}_p$ and τ such as

$$V \cong KT\left(\frac{\Delta \ln \dot{\gamma}_p}{\Delta \tau}\right). \tag{4}$$

Eq. (4) shows that V can be extracted from an experiment where one measures the increase in stress induced by a change in the strain rate by a known factor. The shear stress, τ, is given by the ratio of the measured uniaxial tensile stress, σ, to the Taylor's factor, M, where Taylor's factor is 3 for bcc structures [15,17].

4. Results and discussion

The optical microscopy observation in Fig. 1 shows the interparticles boundaries of the ODS EUROFER97 particles in the plate (Fig. 1(a)) after an etching time of 15 s. The particle size distribution is observed to be in the range of 40–80 μm. The prior austenitic grain boundaries in the EUROFER97 particles are clearly observed as shown in Fig. 1(b) for an etching time of 30 s. The grain size ranges from 2 to 5 μm both in plate and the rod. There is no difference in the particle size and shape and grain size and shape for the parallel and perpendicular direction of rolling.

Fig. 2(a) shows the microstructure of the ODS EUROFER97. The material presents the typical morphology of tempered martensite with low dislocation density and few chromium carbides of the type Cr23C6, having sizes ranging from 100 to 200 nm are found. Yttria particles with the size ranging from 5 to 30 nm was observed and is found to be homogeneously distributed in the matrix of EUROFER97. Fig. 2(b) shows a TEM dark field image, where the yttria particles are observed as white dots. It appears that only part of them is lit, while the rest is invisible or dark. The mean particle size of the yttria particle is calculated and found to be about 8 nm.

Fig. 3(a) and (b) shows the temperature dependence of yield stress and ultimate tensile stress of the ODS EUROFER97 and the as-received EUROFER97, respectively. The strength of the ODS EUROFER97 remains higher than the one of the as-received EUROFER97 up to 600 °C. However, the strength of ODS above 500 °C degrades as well. Both EUROFER97 and ODS tend to follow the same characteristic drop in strength above 500 °C. Fig. 4(a) and (b) shows the uniform and total elongation versus temperature of ODS and of the EUROFER97, respectively. The uniform elongation of the ODS shows a minimum at 500 °C and its elongation is higher than EUROFER97 above 600 °C. However, EUROFER97 shows higher total elongation than ODS at temperatures above 400 °C.

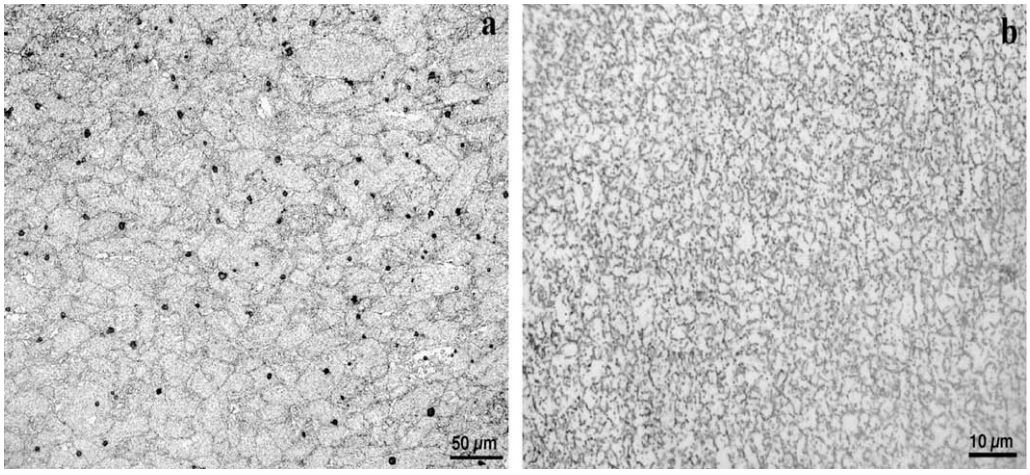

Fig. 1. Optical microstructure of the ODS EUROFER97 for an etching time of 15 s (a) and 30 s (b).

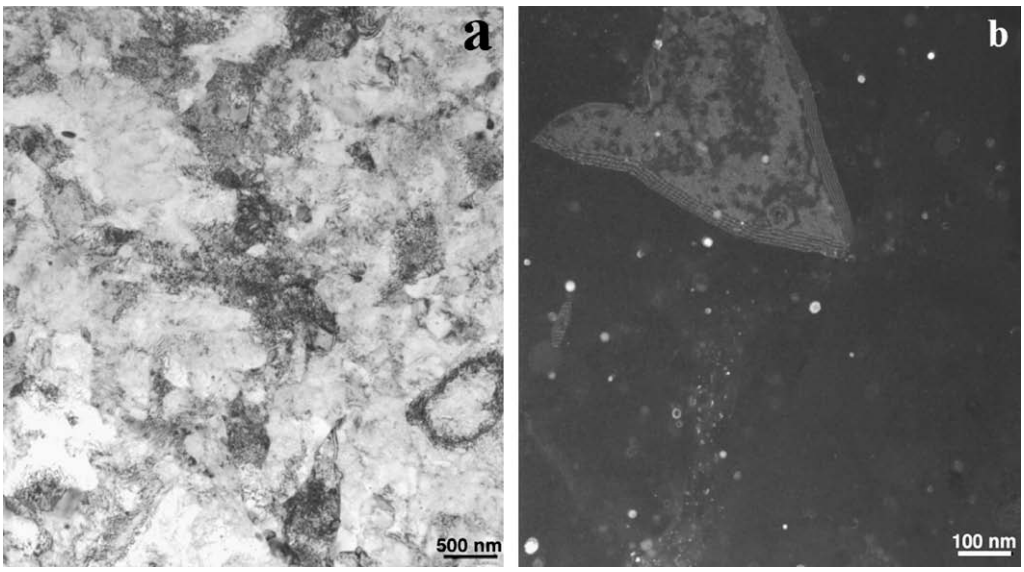

Fig. 2. TEM bright field (a) and dark field image (b) of ODS EUROFER97.

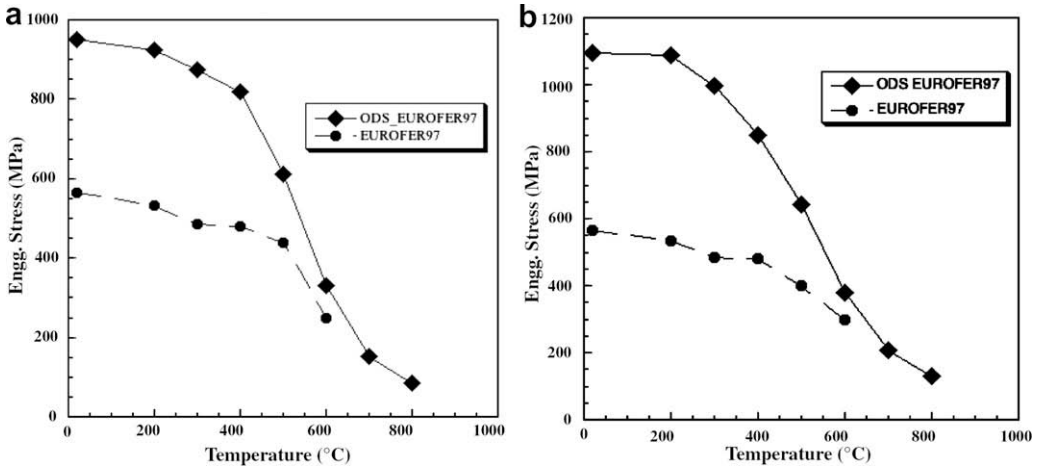

Fig. 3. Tensile yield stress (a) and ultimate tensile stress (b) as a function of testing temperature of EUROFER97 and ODS EUROFER97.

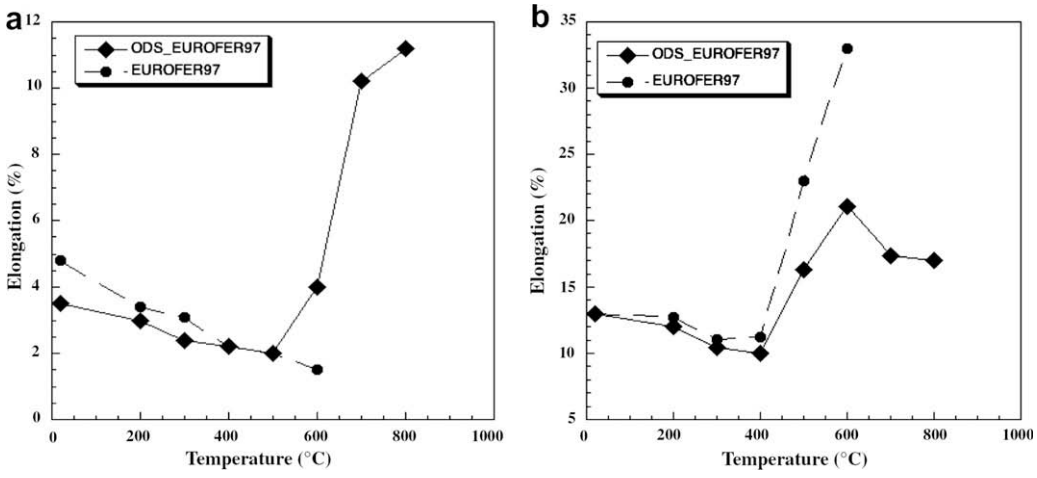

Fig. 4. Uniform elongation (a) and total elongation (b) as a function of testing temperature of EUROFER97 and ODS EUROFER97.

The evolution of the microstructure with increasing temperature as observed in the TEM in situ heating experiment. The changes in the microstructure, especially the disappearance of chromium carbides ($Cr_{23}C_6$) above 800 °C, due to phase change from tempered martensite to austenite was observed. Fig. 5 shows the evolution of the yttria dispersion with increasing temperature as observed in the TEM in situ heating experiment. It appears that yttria particles are very stable over the whole investigated temperature range, without any change in shape or size. It should be noted that yttria particles are often observed to be aligned in rows [16]. This alignment could be due to the hot rolling, whereby all particles follow the direction of the rolling.

Fig. 6(a)–(c) shows the microstructure of EUROFER97 in as-received condition, after heat treatment at 600 and 800 °C, respectively. The material presents in all cases the morphology typical of tempered martensite, with a low dislocation density and martensite laths. Few chromium carbides of the type Cr23C6, having sizes ranging from 100 to 200 nm are observed. There is no clearly visible change in the microstructure of the material up to 800 °C, however there is a small decrease in the density of the dislocation, when compared to the low temperature heat treatment.

Fig. 7(a) and (b) shows the stress–strain curves as a function of temperature and strain rate at room temperature and 800 °C, respectively. The applied strain rates are about 10^{-3} s^{-1} and 10^{-5} s^{-1}. No significant rate-hardening is observed at room temperature (Fig. 7(a)) whereas significant rate-hardening is observed at (Fig. 7(b)) and above 500 °C. Fig. 8(a) and (b) shows the yield stress and ultimate tensile stress, respectively, of ODS EUROFER97 as a function of temperature for the two strain rates. The increase in the stress as the function of the strain rate is less than 5% up to 400 °C and with further increase in temperature it increases up to 80% at 800 °C.

Eq. (3) has been used to calculate the activation volume (V). Fig. 9 shows the activation volume as a function of temperature. It appears that there is a decrease in the activation volume from room temperature to 400 °C, which is less than 3%. At about 500 °C there is a sudden drop in the activation volume that reaches a minimum at 600 °C. With further increase in temperature, there is a significant raise in the activation volume. This abrupt decrease between 400 and 600 °C indicates a change in dislocation-rate controlling mechanism. Up to about 400 °C, the temperature dependence of the yield stress mainly reflects the variation with temperature of the elastic constants as well as the weakly thermally activated dislocation–dislocation and dislocation–particle rate controlling processes [17]. As the temperature increases above 400 °C, a much more pronounced temperature dependence of the yield stress was observed that is likely to be due to a thermally activated mechanism. Note that it is believed the transition occurs between 400 and 600 °C due to the coexistence of both deformation mechanisms, which are referred to as I and II, respectively.

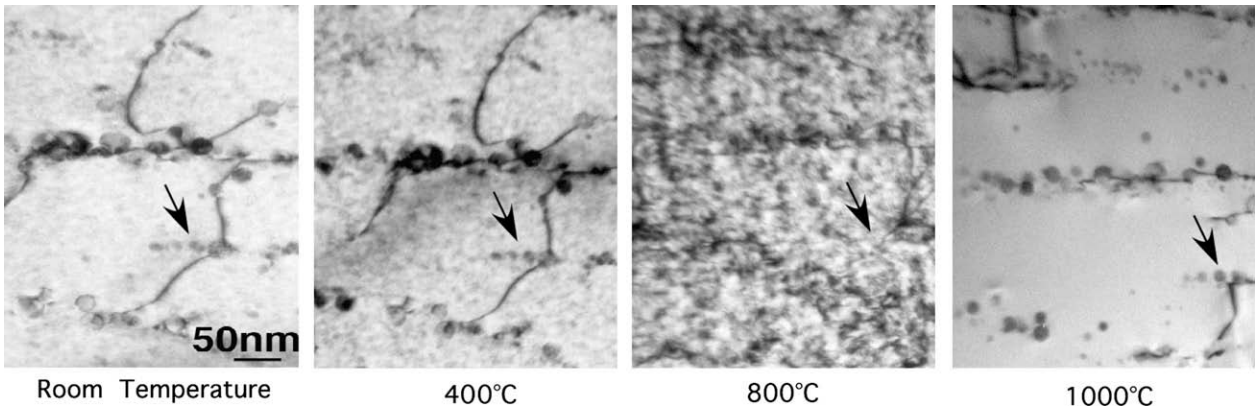

Fig. 5. TEM bright field image of ODS yttria as a function of temperature observed during in-situ heating.

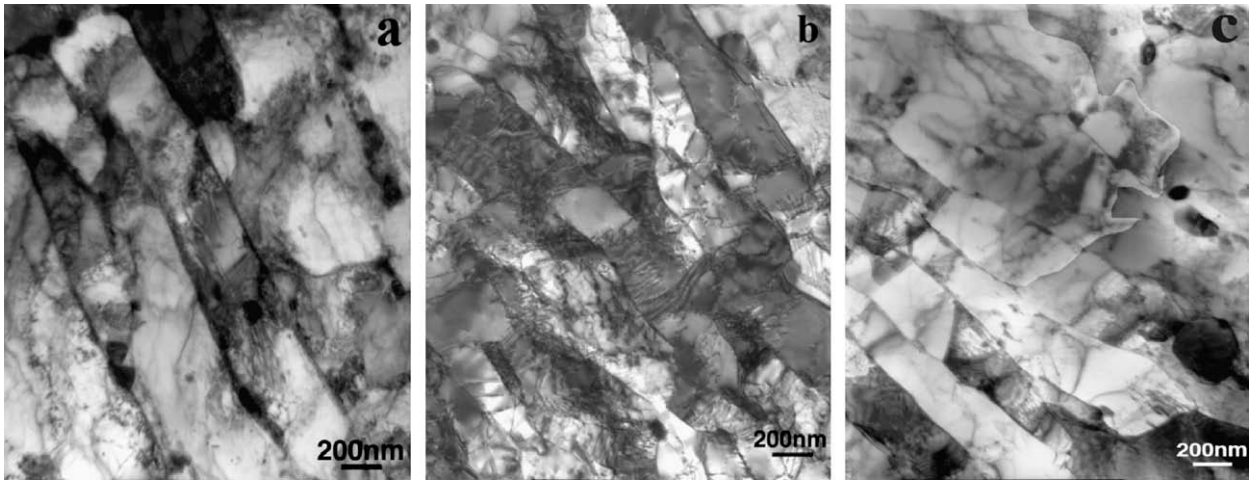

Fig. 6. TEM bright field image of EUROFER97 (a) as-received, EUROFER97 heat treated at (b) 600 °C and (c) 800 °C.

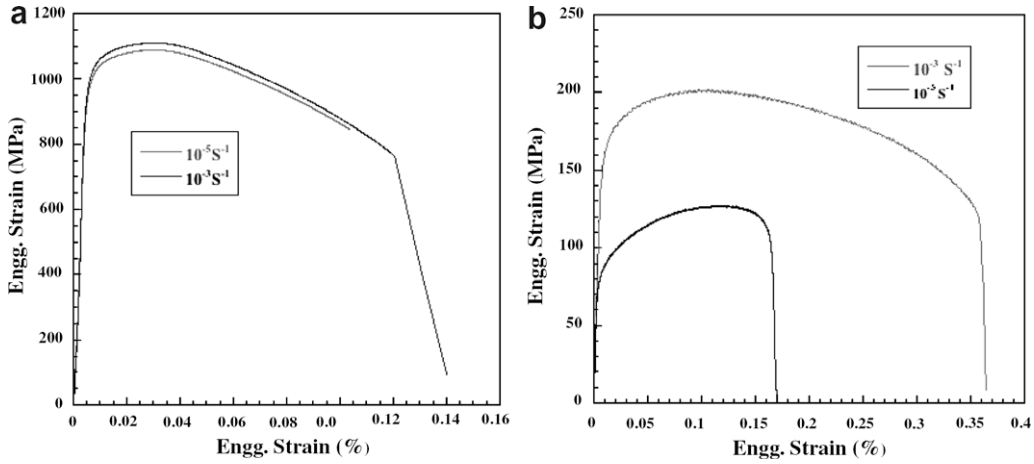

Fig. 7. Stress–strain curve of the tensile test at room temperature (a) and at 800 °C (b) as a function of two different strain rates.

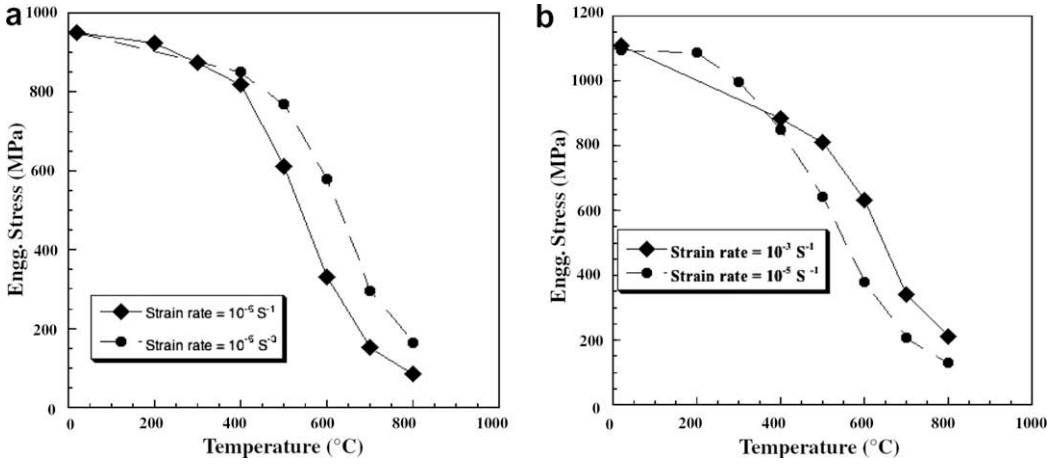

Fig. 8. Yield stress (a) and ultimate tensile stress (b) of ODS EUROFER97 as function of temperature and strain rates.

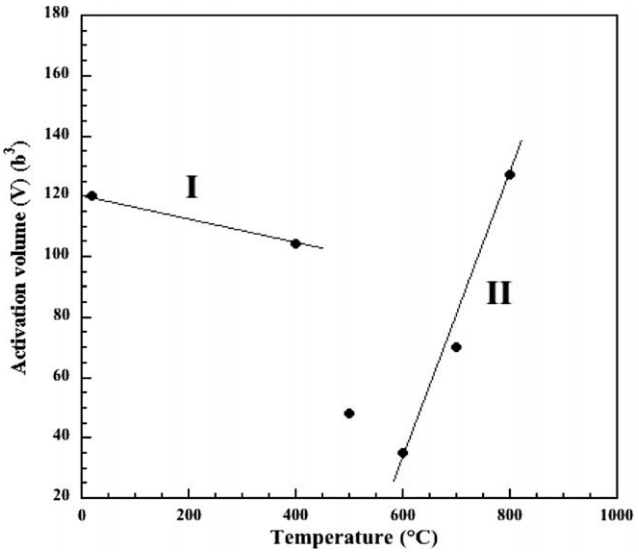

Fig. 9. Temperature dependence of activation volume in ODS EUROFER97.

Fig. 10(a) and (b) presents the averaged yield shear stress and temperature dependence of the activation volume V in the high temperature regime II. At 600 °C, the activation volume is small, typically 35–40b^3, and increases with increasing temperature. It reaches a maximum at 800 °C with typical values from 130 to 140b^3.

In first approximation, the activation energy can be calculated by the integration of the activation volume with respect to the shear stress. Eq. (5) below is used to calculate the activation energy (ΔG) [11,12],

$$\Delta G = \int V \partial\tau + \text{constant}, \tag{5}$$

where V is the activation volume and τ is shear stress. Practically, ΔG was obtained by calculating the area below the fit in Fig. 10(a) and by imposing a linear relationship between ΔG and T so that $\Delta G = 0$ at $T = 0$ K [17]. Fig. 11 shows the activation energy dependence on temperature and shear stress calculated with Eq. (5) between 600 and 800 °C. ΔG calculated varies from 3.5 eV to 4.5 eV from 600 to 800 °C, respectively. Fig. 10(b) presents the stress temperature dependence of the activation energy together with the temperature dependence of the yield stress.

The observed high values of the activation energies might be representative of a dislocation-rate controlling mechanism in which dislocation climb is involved in the overcoming of the obstacles. In real case, vacancies diffuse to the dislocation line and climb occurs along the short segment of the dislocation line. This results

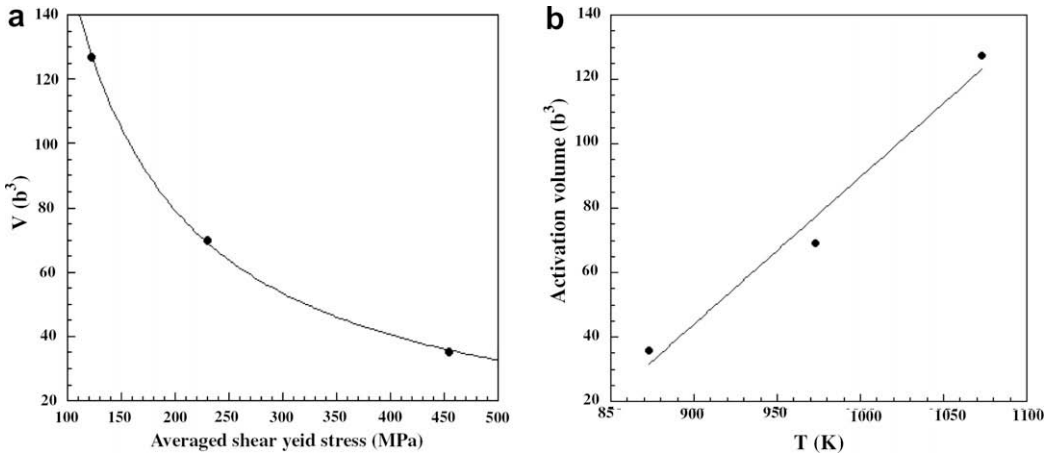

Fig. 10. Average shear stress (a) and temperature (b) dependence of activation volume in ODS EUROFER97.

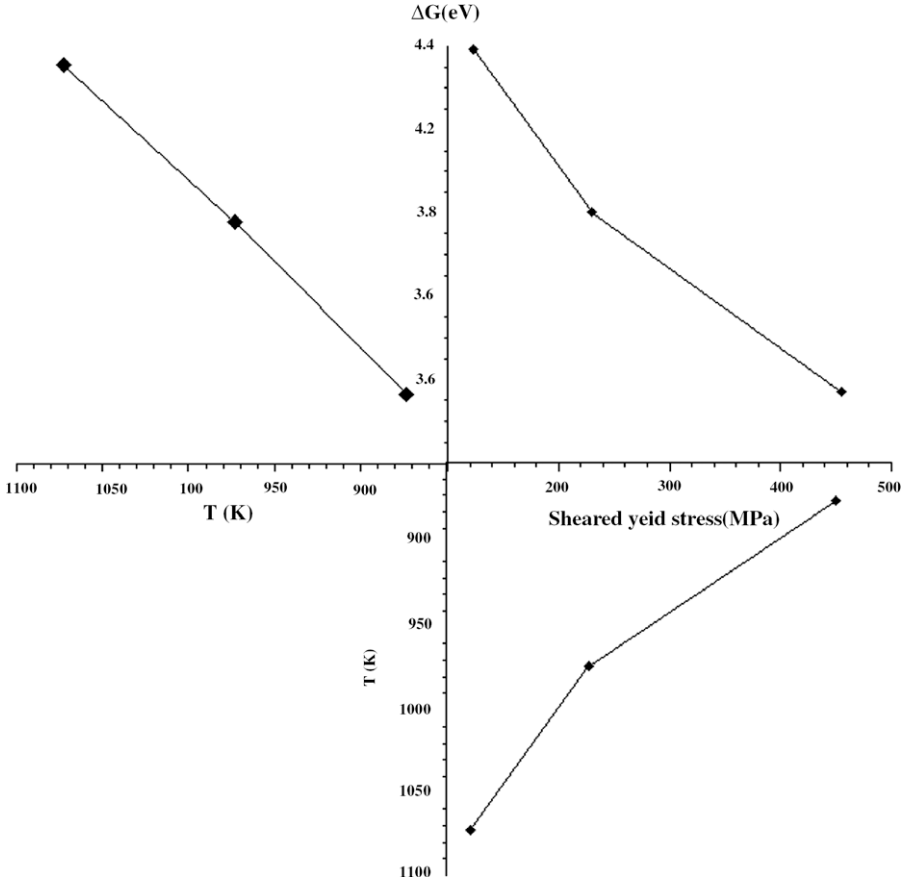

Fig. 11. Stress dependence of the activation energy as the function of the yield stress and temperature.

in the formation of jogs along the dislocation line. Climb proceeds by the nucleation and motion of jogs. The activation energy for the nucleation of a jog is about 1 eV and the activation energy for climb is given by the following equation [13]:

$$U_c = U_j + U_v + U_m, \tag{6}$$

where U_c is the activation energy for climb; U_j is the activation energy for the nucleation of a jog; U_v is the formation energy of a vacancy and U_m is the activation energy for the motion of the vacancy. The calculated value for the vacancy formation and the migration in iron is 1.657 eV and 0.768 eV [14]. With the previous values, the calculated energy U_c, for a dislocation to climb is about 3.5 eV.

While the experimental value is somewhat higher than the calculated one, both values are quite similar. The calculated ΔG value suggests that the deformation mechanism at high temperature could be due to climb of the moving dislocation over the yttria particles, which results in a higher activation energy than the one for pure dislocation climb. The experimental and the calculated values coincide very well with each other. Thus, the calculated ΔG value shows that the deformation mechanism at high temperature could

be due to climb of the moving dislocation over the obstacle for a constant microstructure as observed during the in situ TEM heating experiment up to 800 °C and also with the microstructural analysis upon heat treatment up to 800 °C.

5. Conclusion

The mechanism involved during the high temperature deformation in ODS EUROFER97 steels is analyzed.

ODS EUROFER97 as received plate has a tempered martensite microstructure and the dispersed yttria particles were found to be homogeneously distributed in the matrix. The mean particle size of yttria is 8 nm.

EUROFER97 ODS steel shows higher strength than base material up to about 650 °C. Higher uniform elongation at temperatures above 600 °C, was observed in ODS than in EUROFER97. Higher total elongation was observed in EUROFER97 than ODS for temperatures above 400 °C.

In situ TEM observation shows that the yttria particles are very stable up to 1000 °C. No visible changes neither in the microstructure nor in the yttria particles was observed up to 800 °C. No visible changes in the general microstructure of the EUROFER97 were observed for all heat treatments up to 800 °C.

Transition between two rate controlling mechanisms occurs at about 500 °C as indicated by the discontinuity in the activation volume. Large activation energy of the rate controlling mechanism (3.5–4.5 eV) was calculated. Such a value was found consistent with activation energy for dislocation climb-controlled mechanism to overcome obstacles.

Acknowledgements

The Paul Scherrer Institute is acknowledged for the overall use of the facilities.

This work, supported by the European Communities under the contract of Association between EURATOM/Confédération Suisse was carried out within the framework of the European Fusion Development Agreement. The views and opinions expressed herein do not necessarily reflect those of the European Commission.

References

[1] D.K. Mukhopadhyay, F.H. Froes, D.S. Gelles, J. Nucl. Mater. 258–263B (1998) 1209.
[2] G.R. Romanoski, L.L. Snead, R.L. Klueh, D.T. Hoelzer, J. Nucl. Mater. 283–287A (2000) 642.
[3] R. Schäublin, T. Leguey, P. Spätig, N. Baluc, M. Victoria, J. Nucl. Mater. 307–311 (2002) 778.
[4] S. Ukai, M. Harada, H. Okada, M. Inoue, S. Nomura, S. Shikakura, K. Asabe, T. Nishida, M. Fujiwara, J. Nucl. Mater. 204 (1993) 65.
[5] V.V. Sagaradze, V.I. Shalaev, V.L. Arbuzov, B.N. Goshchitskii, Yun Tian, Wan Qun, Sun Jiguang, J. Nucl. Mater. 295 (2&3) (2001) 265.
[6] R. Lindau, A. Möslang, M. Schirra, P. Schlossmacher, M. Klimenkov, J. Nucl. Mater. 307–311 (2002) 769.
[7] R.L. Klueh, D.R. Harries, ASTM Publication, 2001.
[8] R.H. Jones, H.L. Hensich, K.A. McCarthy, J. Nucl. Mater. 271&272 (1999) 518.
[9] R. Schäublin, M. Victoria, J. Nucl. Mater. 283–287 (2000) 339.
[10] J.W. Christian, B.C. Masters, Proc. Roy. Soc. A 281 (1964) 233.
[11] G. Schoeck, Phys. Status Solidi 8 (2) (1965) 499.
[12] M. Cagnon, Philos. Mag. 24 (1971) 1465.
[13] G.E. Dieter, Mechanical Metallurgy, McGraw Hill, 1988.
[14] S. Xiaolin, W. Chongyu, Physica B 344 (2004) 413.
[15] P. Spätig, J. Bonneville, J.L. Martin, Mater. Sci. Eng. A 167 (1993) 73.
[16] R. Schäublin, T. Leaguey, M. Victoria, J. Nucl. Mater. 307–311 (2002) 778.
[17] P. Spätig, G.R. Odette, G.E. Lucas, J. Nucl. Mater. 275 (1999) 324.